Quantal Release of ATP in Mouse Cortex

Yuriy Pankratov, Ulyana Lalo, Alexei Verkhratsky, and R. Alan North

Faculty of Life Sciences, University of Manchester, Manchester M13 9PT, UK

Transient currents occur at rest in cortical neurones that reflect the quantal release of transmitters such as glutamate and γ-aminobutyric acid (GABA). We found a bimodal amplitude distribution for spontaneously occurring inward currents recorded from mouse pyramidal neurones in situ, in acutely isolated brain slices superfused with picrotoxin. Larger events were blocked by glutamate receptor (AMPA, kainate) antagonists; smaller events were partially inhibited by P2X receptor antagonists suramin and PPADS. The decay of the larger events was selectively prolonged by cyclothiazide. Stimulation of single intracortical axons elicited quantal glutamate-mediated currents and also quantal currents with amplitudes corresponding to the smaller spontaneous inward currents. It is likely that the lower amplitude spontaneous events reflect packaged ATP release. This occurs with a lower probability than that of glutamate, and evokes unitary currents about half the amplitude of those mediated through AMPA receptors. Furthermore, the packets of ATP appear to be released from vesicle in a subset of glutamate-containing terminals.

The Journal of General Physiology

INTRODUCTION

An elementary event of synaptic transmission is a spontaneous release of packet or quantum of transmitter. At the neuromuscular junction this corresponds to the acetylcholine content of a single vesicle (Katz and Miledi, 1963), although in the central nervous system the situation is more complex (Redman, 1990; Auger and Marty, 2000). Such spontaneous neurotransmitter release is manifest electrically by miniature excitatory postsynaptic currents (mEPSCs) and miniature inhibitory postsynaptic currents (mIPSCs). In the mammalian central nervous system, the transmitters producing mEPSCs and mIPSCs are thought to be almost exclusively glutamate and γ-aminobutyrate (GABA).

Ionotropic P2X receptors, at which extracellular ATP directly gates a cation-permeable channel, are widely expressed throughout the central nervous system (Collo et al., 1996; Verkhratsky et al., 1998; Norenberg and Illes, 2000; Verkhratsky and Steinhauser, 2000; Khakh, 2001; North, 2002; North and Verkhratsky, 2006). Evoked synaptic transmission mediated by ATP acting at P2X receptors has been reported in several regions of CNS in situ, including medial habenula (Edwards et al., 1992; Edwards et al., 1997), hippocampus (Pankratov et al., 1998; Mori et al., 2001), locus coeruleus (Nieber et al., 1997), dorsal horn (Bardoni et al., 1997; Jo and Schlichter, 1999), and cerebral cortex (Pankratov et al., 2002, 2003). However, the amplitude of the evoked synaptic currents remaining after block of glutamate receptors (and presumed to be purinergic) is typically very small; some 5–15% of that of the initial unblocked current. The identification of such evoked synaptic currents has been hampered by their small amplitude and lack of highly selective P2X receptor blockers.

Mechanisms of ATP release have proved controversial, with proposals including mechanical deformation, gap junction hemichannels (Pearson et al., 2005), or the chloride channels of the cystic fibrosis conductance regulator (for review see Sperlagh and Vizi, 2001). However, any central neurotransmitter role for ATP should be associated with the quantal release of ATP-storing vesicles, as was originally reported for the release of ATP from sympathetic nerves (Burnstock and Holman, 1961). In neurones cultured from the lateral hypothalamus of the embryonic chick or neonatal mouse, spontaneous mEPSCs have also been observed in the presence of blockers of glutamate and GABA receptors (Jo and Role, 2002). Similarly ATP-mediated mEPSCs were occasionally detected in neurones from medial habenula (Edwards et al., 1997). Nevertheless, there has been no biophysical analysis of such events, no systematic reports of their occurrence in intact neuronal tissue and, more crucially, no effort to determine whether they correspond to the unitary events underlying evoked purinergic transmission. The purpose of the present experiments was to test the hypothesis that ATP was released from vesicles in the cerebral cortex, and to measure the quantal parameters of ATP-mediated component of evoked and spontaneous EPSCs.

Correspondence to R. Alan North: alan.north@manchester.ac.uk

Abbreviations used in this paper: CNQX, 6-cyano-7-nitroquinoxaline-2,3-dione; D-APV, D-2-amino-5-phosphonovalerate; GABA, γ-aminobutyric acid; eEPSC, evoked excitatory postsynaptic current; mEPSC, miniature EPSC; NBQX, 2,3-dihydroxy-6-nitro-7-sulfamoylbenzo(f)quinoxaline; PPADS, pyridoxaphosphate-6-azophenyl-2'-4'-disulphonic acid; SYM2081, [2S,4R]-4-methylglutamic acid.

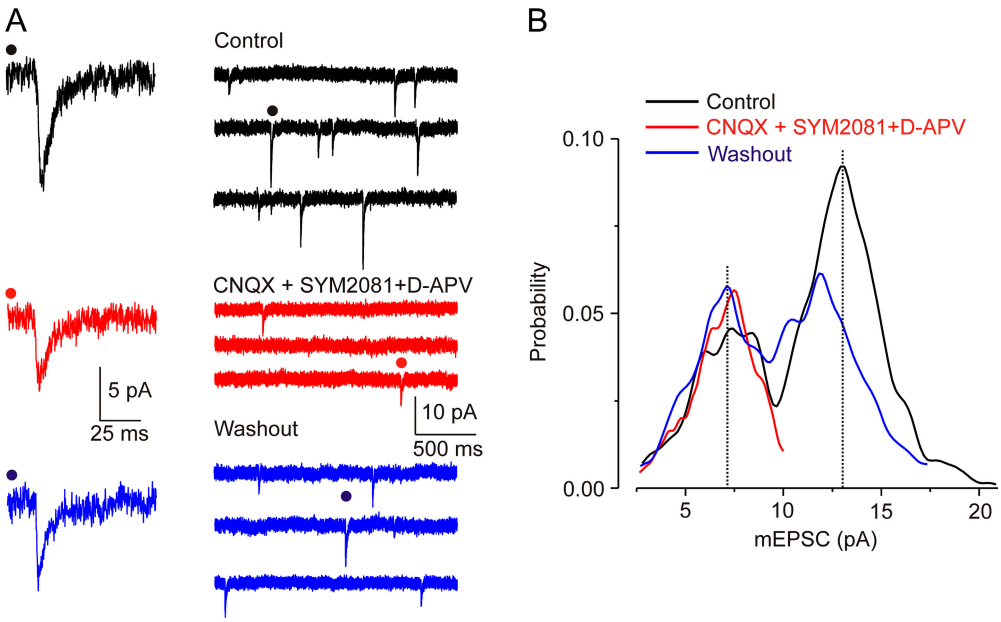

Figure 1. Two populations of mEPSC amplitudes. (A) Control mEPSCs in TTX (1 μM) and picrotoxin (100 μM), after addition (red) and washout (blue) of CNQX (50 μM), SYM2081 (3 μM), and D-APV (30 μM). (B) Amplitude histogram of mEPSCs from the cell shown in A. Note the disappearance of the larger peak after the inhibition of glutamate receptors (red) and washout (blue).

MATERIALS AND METHODS

Electrophysiology

CBL57 mice (15–45-d-old) were killed according to UK legislation. Brains were removed rapidly and placed into ice-cold saline (in mM) NaCl 138, KCl 3, $CaCl_2$ 0.5, $MgCl_2$ 2.5, NaH_2PO_4 1, $NaHCO_3$ 25, glucose 15, pH 7.4 gassed with 95% O_2–5% CO_2. Transverse slices (~300 μm) were kept for 1–4 h before recording at 22–24°C, in the above solution but with (in mM) $CaCl_2$ 2.5, $MgCl_2$ 1. Somatosensory cortex layer 2/3 neurones with pyramidal shaped somata were selected using an infrared differential interference contrast optics, and recordings were made with patch pipettes (4 MΩ) filled with (in mM) 50 KCl, 55 K-gluconate, 10 NaCl, 10 HEPES, 2 MgATP, 0.1 EGTA, pH 7.35. In some experiments, the intracellular solution was used to set the chloride reversal potential at −60 mV; it contained (in mM) 3 CsCl, 102 Cs-gluconate, 10 NaCl, 10 HEPES, 2 MgATP, 0.1 EGTA, pH 7.35. The membrane potential was set at −80 mV unless stated otherwise. Junction potentials were nulled with an open electrode in the recording chamber before each experiment. The series and the input resistances were 4–12 MΩ and 500–1,300 MΩ, respectively; in cells accepted for analysis these varied by <20%.

EPSCs were evoked by stimulating axons originating from layer V neurones with a bipolar glass electrode (2–3-μm tip diameter) containing extracellular solution. The electrode was placed in layer V close to the layer IV border, stimulus duration was 100 μs, and the frequency was 0.3 Hz. The intensity was set either at a minimal level (10–20% higher in intensity than threshold at which EPSC appeared; typically 0.7–1.2 μA) or at a stronger level (evoked EPSCs with amplitude two to four times greater than those evoked by minimal stimulation, but also failures in at least 10–20% of trials, typically 1.5–3 μA). Minimal level stimulation was set to meet the criteria of single-axon stimulation (Yoshimura et al., 2000) including all-or-none synaptic response, little variation in EPSC latencies, and absence of change in the mean size or shape of the EPSC with 20–50% increase in stimulus intensity. Hence minimal stimulation most likely activates a single fiber (Yoshimura et al., 2000; Rubio and Soto, 2001) whereas stronger stimulation would presumably activate several axons.

Spontaneous miniature excitatory synaptic currents (mEPSCs) were recorded in tetrodotoxin (1 μM) and picrotoxin (100 μM), except where stated. Currents were monitored using an EPC-9 amplifier (HEKA), filtered at 3.9 kHz, and digitized at 10 kHz. Experiments were controlled by PULSE/PULSEFIT software (HEKA) and data were analyzed by self-designed software.

Data Analysis

Quantal analysis of evoked synaptic currents was as previously described (Pankratov and Krishtal, 2003). Spontaneous inward currents of amplitude higher than two SD of baseline noise were selected, each analyzed in a 140-ms window (40 ms before and 100 ms after peak). The mEPSC peak amplitude was determined using a computer routine based on the fitting of each current trace by the model curve with single exponential rise and decay phases. The minimal square root procedure was used to determine the amplitude of the model curve, while the time constants and offset were optimized by the gradient method to minimize the mean square error. The mean square error of the fit was <25% amplitude. A set of 800–1,500 mEPSCs or EPSCs was recorded and used for statistical analysis in each cell tested. Amplitude distributions were analyzed with probability density functions and likelihood maximization techniques (Stricker et al., 1996a,b). The distributions of amplitude and decay time of spontaneous mEPSCs were fitted with bimodal function consisting with variable peak location, width, and amplitude, and weights were calculated as the integrals of the corresponding Gaussian functions. Amplitude distributions of evoked EPSCs were fitted with multiquantal binomial or single-quantal models comprising two Gaussian functions, with one peak location fixed at zero and the second variable peak.

RESULTS

Two Populations of mEPSCs

Amplitudes of mEPSCs showed a clear bimodal distribution with peaks at 7.1 ± 2.9 and 13.4 ± 4.8 pA (Fig. 1); in all 61 neurones this was best fit by two Gaussians (maximum likelihood method, $P < 0.05$). The overall mean amplitude (in 1 μM tetrodoxin and 100 μM picrotoxin) was 11 ± 4 pA ($n = 61$), and the frequency

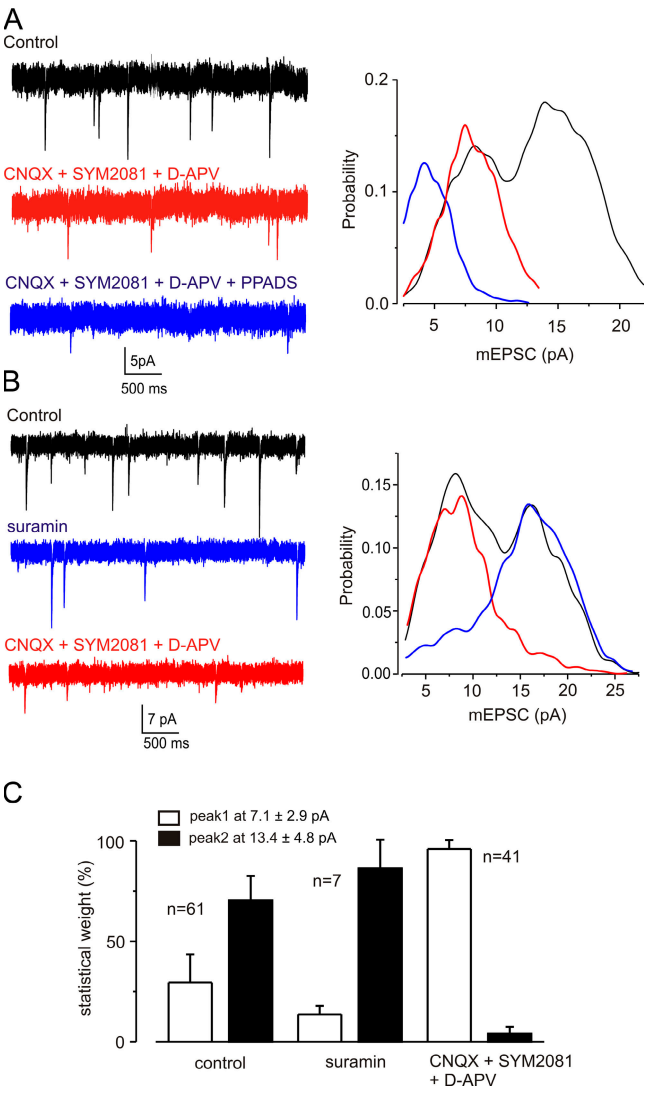

Figure 2. Selective block of high and low amplitude mEPSCs. (A) mEPSCs in control conditions, in CNQX (50 μM), SYM2081 (10 μM), and D-APV (30 μM, 5 min; red), and after the further addition of PPADS (3 μM, 5 min; blue). Right panel shows distributions of mEPSC amplitudes. Glutamate receptor blockade removed the high amplitude mEPSCs (red), and subsequent addition of PPADS reduced the amplitude of the remaining mEPSCs (blue). (B) mEPSCs in control conditions, in suramin (10 μM, 5 min; blue), and after further addition of CNQX (50 μM), SYM2081 (10 μM), and D-APV (30 μM, 5 min; red). Right panel shows distributions of EPSC amplitudes. Note that suramin blocked the lower amplitude mEPSCs (blue), and subsequent addition of glutamate receptor blockers strongly reduced the occurrence of the larger mEPSCs (red). (C) Summary of the differential sensitivity of low- and high-amplitude mEPSCs to suramin and ionotropic glutamate receptor antagonists. All recordings were made in TTX (1 μM) and picrotoxin (100 μM).

was 1.6 ± 0.7 Hz (n = 61; Fig. 1 A). The high-amplitude mEPSCs were selectively and reversibly blocked by glutamate receptor antagonists (AMPA/kainate receptor blockade: 50 μM 6-cyano-7-nitroquinoxaline-2,3-dione [CNQX]; NMDA receptor blockade: 30 μM D-2-amino-5-phosphonovalerate [D-APV]; kainate receptor desensitization: 10 μM [2S,4R]-4-methylglutamic acid [SYM2081]; Fig. 1 B; we used a mixture of several ionotropic glutamate receptors antagonists and kainate receptor desensitizing agent SYM2081 to ascertain complete inhibition of glutamate transmission). In this antagonist cocktail, mEPSCs of lower amplitude were observed in 41 of the 45 cells at 0.49 ± 0.28 Hz; their mean amplitude (7.6 ± 2.8 pA) was the same as that of the lower peak of the control bimodal distribution; their amplitude was unchanged even in a higher CNQX concentration (100 μM; n = 8). Selective inhibition of the higher amplitude mEPSCs was also observed with (a) AMPA/kainate receptor blocker 2,3-dihydroxy-6-nitro-7-sulfamoyl-benzo(f)quinoxaline (NBQX, 100 μM) and D-APV (30 μM), n = 8; (b) CNQX (50 μM) and the nonspecific glutamate receptor blocker kynurenic acid (2 mM), n = 5; and (c) the noncompetitive AMPA receptor (±)-4-(4-aminophenyl)-1,2-dihydro-1-methyl-2-propylcarbamoyl-6,7-methylenedioxyphthalazine (SYM 2206, 50 μM) with SYM2081 (10 μM) and D-APV (30 μM), n = 7. These results strongly suggest that the residual low amplitude population of mEPSCs does not involve ionotropic glutamate receptors.

The low-amplitude mEPSCs were partially inhibited by PPADS (3 μM, Fig. 2 A) and suramin (10 μM, Fig. 2 B), which both block most of P2X receptor subtypes (North and Surprenant, 2000). PPADS (3 μM) reduced the amplitude (by 24 ± 16%, n = 14) and frequency (by 43 ± 27%, n = 8) of low-amplitude mEPSCs. When suramin was washed out and replaced by glutamate receptor blockers (CNQX, SYM2081, and D-APV), the low-amplitude mEPSCs reappeared and the higher amplitude events were blocked (Fig. 2, B and C). When added in the presence of NBQX and D-APV, suramin (10 μM) also reduced the amplitude (by 55 ± 8%, n = 7) and frequency (47 ± 24%, n = 7) of the low-amplitude residual mEPSCs (unpublished data). This effect was mimicked by the suramin analogue 8,8'-(carbonylbis(imino-4,1-phenylenecarbonylimino-4,1-phenylenecarbonylimino)) bis(1,3,5-naphthalenetrisulfonic acid) (NF279, 1 μM; see Rettinger et al., 2000), which also substantially blocked the residual mEPSCs when added in the presence of NBQX and D-APV; the amplitude of mEPSCs was reduced by 31 ± 9% and their frequency by 44 ± 20% (n = 5). 8-Cyclopentyl-1,3-dipropylxanthine (DCPCX, 1 μM; an adenosine A_1 receptor antagonist) and hexamethonium (100 μM; a nicotinic receptor blocker) had no effect on the mEPSCs.

Cyclothiazide reduces desensitization of AMPA receptors (Partin et al., 1993). Cyclothiazide (50 μM) prolonged the decay of a subset of mEPSCs (Fig. 3). Thus, in cyclothiazide the distribution of τ_{decay} changed from unimodal to bimodal (Fig. 3 C; τ_{decay} 8.9 ± 1.6 and 16.8 ± 2.5 ms, n = 5). The time constants of rise and decay

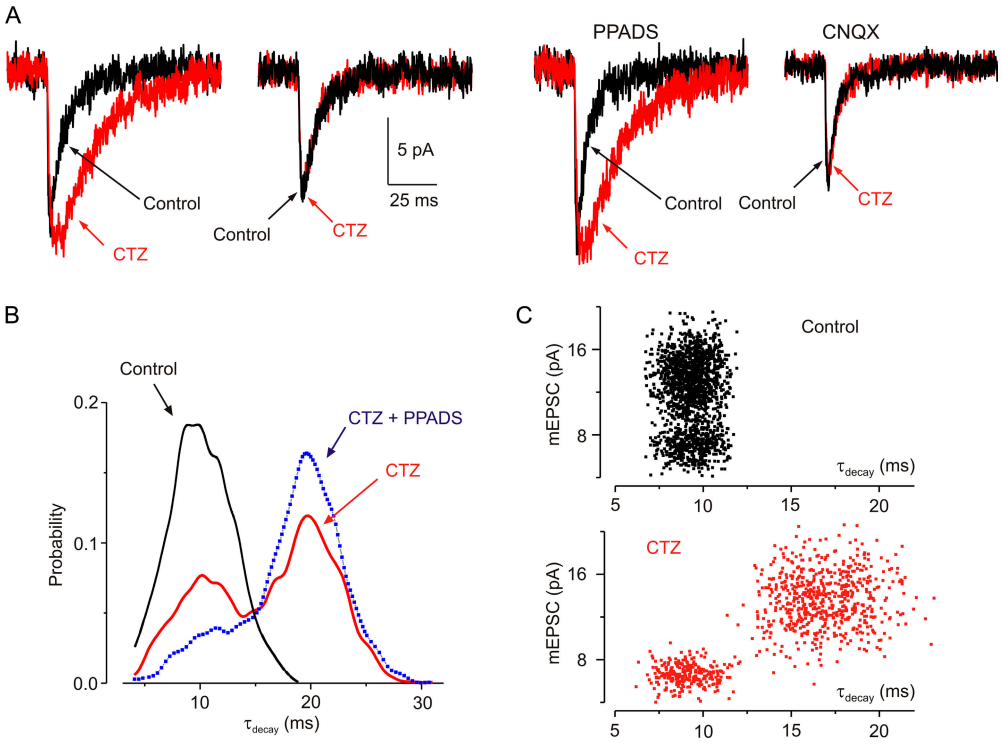

Figure 3. Cyclothiazide selectively prolongs larger mEPSCs. (A) A large mEPSC that is markedly prolonged by cyclothiazide (50 μM, red) and a smaller mEPSC that is unaffected by cyclothiazide. In PPADS (3 μM), cyclothiazide (50 μM) increased the duration of all mEPSCs, but in CNQX (50 μM), cyclothiazide had no effect on mEPSCs. (B) Distribution of decay time constants (τ_{decay}) of mEPSCs. Black, control; red, cyclothiazide (50 μM); Blue, cyclothiazide and PPADS (3 μM). Note the appearance of slowly decaying mEPSCs in cyclothiazide and the selective inhibition of faster decaying mEPSCs by PPADS. (C) mEPSC amplitude vs. decay time constant for control (top, 1,700 events) and cyclothiazide (bottom, 900 events) for five cells. All recordings were in TTX (1 μM) and picrotoxin (100 μM).

of mEPSCs were not affected by CNQX (50 μM; control: τ_{rise} 1.1 ± 0.6 ms, τ_{decay} 9.5 ± 1.9 ms, n = 65 cells; CNQX: τ_{rise} 1.2 ± 0.5 ms and τ_{decay} 9.8 ± 2.1 ms, n = 61 cells), but cyclothiazide did not change the decay of mEPSCs in the presence of CNQX (50 μM; Fig. 3 A). In cyclothiazide, PPADS (3 μM) substantially blocked the rapidly decaying mEPSCs, without much affecting the slower mEPSCs (Fig. 3). We hypothesize from these results that the population of smaller amplitude, cyclothiazide-insensitive mEPSCs are mediated by ATP acting on P2X receptors.

Both populations (low and high amplitude) of mEPSCs were enhanced by α-latrotoxin, which is a potent stimulator of vesicular exocytosis (Ushkaryov et al., 2004); latrotoxin (300 nM, 5–10 min) increased frequency of control mEPSCs by 84 ± 9% (n = 6) and low-amplitude nonglutamatergic mEPSCs by 127 ± 12% (n = 6; unpublished data). Bafilomycin blocks vesicular refilling (Zhou et al., 2000); bafilomycin (1 μM, 2 h) reduced the frequency of mEPSC in control conditions by 95% (n = 4) and completely eliminated the low-amplitude mEPSC in four cells tested.

ATP mEPSCs Are Independent of Glutamate and GABA Release

The asynchrony between the two populations of mEPSCs indicates that the release of ATP and glutamate is unrelated. However, there is evidence from cultured hypothalamic neurones that ATP might be coreleased with GABA (Jo and Role, 2002). To test for the corelease of ATP with GABA, we recorded spontaneous synaptic currents in the presence of CNQX (50 μM) and D-APV (30 μM) but without picrotoxin. We used a cesium gluconate intracellular solution to separate the cationic currents through P2X receptors (reversal potential ~0 mV) and chloride currents through GABA receptors (reversal potential about −60 mV; the extracellular solution contained TTX [1 μM] as well). Spontaneous events at −80 mV (Fig. 4 A) comprised of two types of inward current: one had smaller amplitude (6.9 ± 2.1 pA) and faster decay (τ_{decay} 9.7 ± 1.9 ms; 44 ± 10% of events), and the other larger amplitude (13.8 ± 3.7 pA) and slower decay (τ_{decay} 19.2 ± 5.5 ms; n = 6; 56 ± 11% of events; n = 6 throughout).

At −40 mV, both inward (cationic) and outward (chloride) currents were observed (Fig. 4 A, bottom traces). Inward currents had τ_{decay} of 9.9 ± 2.3 ms; they were resistant to bicuculline and inhibited by PPADS (3 μM: by 26 ± 12%, n = 4). They occurred at 41 ± 13% of the frequency of the events recorded at −80 mV (n = 6). Outward currents had τ_{decay} of 21.1 ± 8.5 ms; they were abolished by bicuculline (30 μM, n = 6). They occurred at 50 ± 15% (n = 6) of the control frequency. Therefore, these two distinct populations of spontaneous events are likely to be mediated by P2X receptors (inward, faster kinetics) and GABA receptors (outward, slower kinetics).

We infer that ATP is not released synchronously with GABA, because the superimposition of inward and outward currents at −40 mV would result in currents of

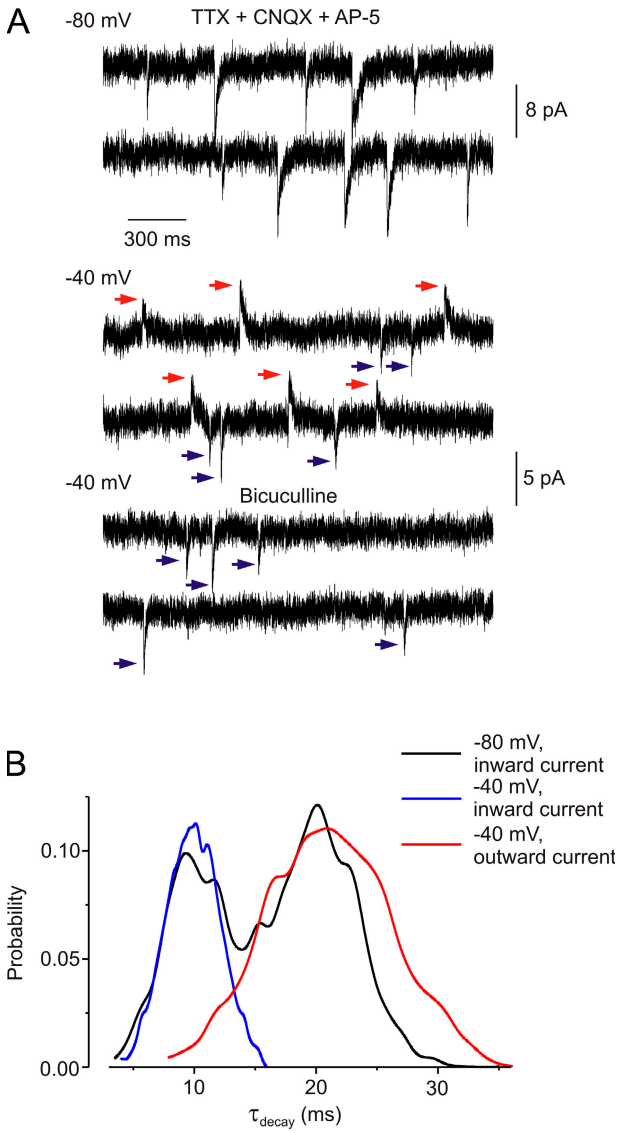

Figure 4. ATP release is asynchronous with GABA release. (A) Representative spontaneous currents recorded in TTX (1 μM), CNQX (50 μM), and D-APV (30 μM), in neurones with cesium-gluconate intracellular solution ($E_{Cl} = -60$ mV). At −80 mV, all currents are inward, but some decay more slowly than others. At −40 mV, GABA-mediated currents are outward (red arrows) and ATP-mediated currents are inward (blue arrows). Bicuculline (30 μM) completely inhibited outward currents. (B) Distribution of inactivation time constants (τ_{decay}) of currents recorded at −80 mV (binominal distribution corresponding to two populations of currents) and at −40 mV. At −40 mV, the outward currents (GABA mediated, red) decay much more slowly than the inward currents (ATP mediated, blue).

very small net amplitude and therefore lead to a decrease in the amplitude and frequency of apparent spontaneous currents. In fact, the sum of the frequencies of fast inward (ATP-mediated) and slow outward (GABA-mediated) mEPSCs recorded at −40 mV was not different from that of all mEPSCs at −80 mV (Fig. 4 B), which is consistent with the hypothesis of non-coordinated release.

Quantal Analysis of Evoked EPSCs

Experiments using receptor antagonists suggested that a small component of the evoked EPSC (eEPSC) in rat cortical neurones results from ATP acting at P2X receptors (Pankratov et al., 2002, 2003). This implies that unitary components of the eEPSC corresponding to the ATP-mediated mEPSC should be detectable at this synapse. Vertical axons originating from layer V neurones were stimulated with either minimal or stronger stimulation (see Materials and methods). Minimal stimulation most likely activated a single fiber providing input to the pyramidal neurone (Gil et al., 1999; Yoshimura et al., 2000), whereas stronger stimulation presumably activated several axons. We recorded excitatory synaptic currents, evoked and spontaneous, first in picrotoxin (100 μM) and D-AP5 (30 μM), which were our control condition and then again after further addition of CNQX (50 μM) and SYM2081 (10 μM; Fig. 5).

The results were of two kinds. In 19 out of 35 cells, the EPSC evoked by minimal stimulation was completely blocked by CNQX and SYM2081 (Fig. 5 A, top). The amplitude distribution of the evoked EPSC had a single peak located at ~4–12 pA (Fig. 5 B, top); it was better fit by a single-quantal model than by a unimodal nonquantal model (confidence level $\alpha < 0.01$, $n = 19$) or a multiquantal binomial model ($\alpha < 0.05$ for 14 of 19 cells). The average quantal size was 9.3 ± 5.2 pA; the difference between quantal size of the unitary evoked EPSC and the mean amplitude of spontaneous glutamatergic mEPSC was not statistically significant ($P > 0.05$, ANOVA test). With stronger stimulation in these cells, eEPSCs were observed in the presence of glutamate receptor antagonists in all 19 cells tested (Fig. 5 B, bottom); these residual eEPSCs were decreased in amplitude by 39 ± 17% in PPADS (10 μM, $n = 4$), similar to previous results (Pankratov et al., 2002, 2003). The eEPSC amplitude distribution exhibited multiple peaks (Fig. 5 B, bottom) and was well fit by a multiquantal binomial model (confidence level $\alpha < 0.05$) for all 19 cells. The maximal number of quanta was 2.4 ± 1.3, the mean quantal content (product of number of quanta and release probability) was 1.4 ± 0.8 ($n = 19$), and the quantal size was 9.2 ± 5.5 pA. This amplitude distribution became single quantal in glutamate receptor antagonists (CNQX, SYM2081; in 14 of 19 cells; Fig. 5 B, bottom). The average quantal size of the residual component was 6.8 ± 2.9 pA; the maximal number of quanta was 1.6 ± 0.9, and the mean quantal content was 0.36 ± 0.15 ($n = 19$). These results indicate that the minimal stimulation results in synaptic transmission at a single synapse that does not have any purinergic component, but that an increase in the stimulus strength recruits further fibers that result in synaptic transmission at additional synapses, some of which do have a purinergic component.

In the second group (16 of 35 cells), the EPSC evoked with minimal stimulation was not completely blocked

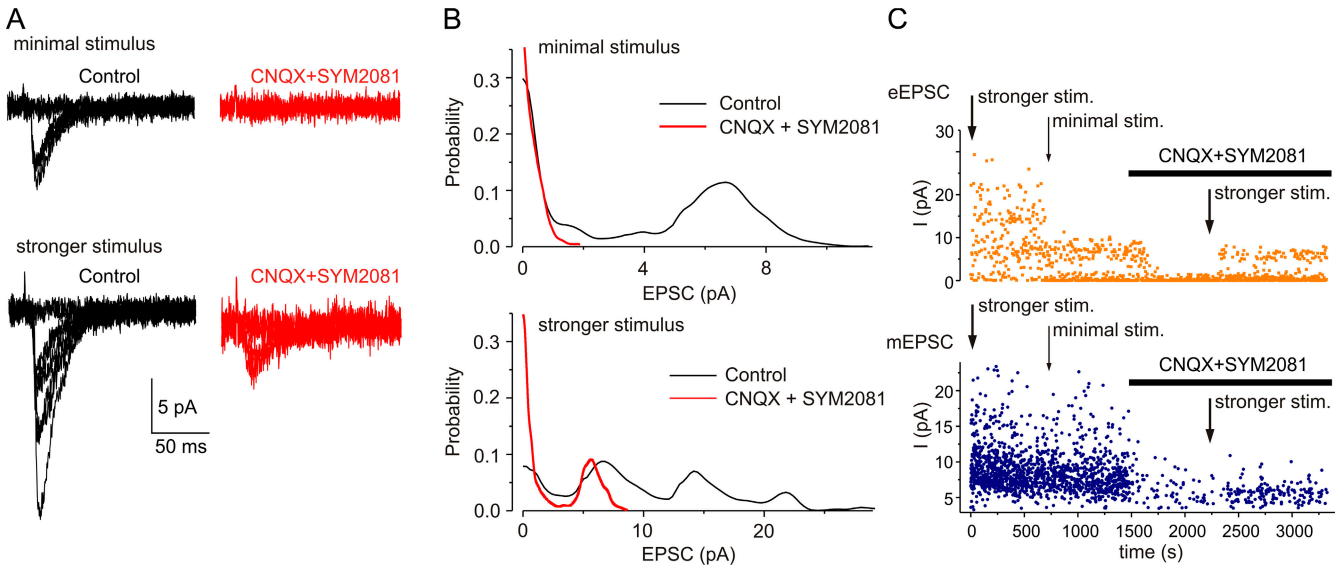

Figure 5. Evoked and spontaneous EPSCs. (A) Minimal stimulation evoked EPSCs, which often fail; these are blocked by CNQX (50 μM) and SYM2081 (10 μM). Stronger stimulation evoked EPSCs, which sometimes fail, but which are incompletely blocked by the glutamate antagonists. (B) Amplitude distributions of the EPSCs evoked by minimal (top panel) and stronger stimulation (bottom panel) before and after adding glutamate receptor blockers (50 μM CNQX and 10 μM SYM2081). (C) Time course of experiment such as illustrated in A. Top graph shows the amplitudes of evoked EPSCs and bottom graph shows amplitudes of spontaneous mEPSCs, recorded in between the stimulations. All in picrotoxin (100 μM) and D-APV (30 μM).

by the glutamate receptor antagonists (Fig. 6 A); the residual current was partially inhibited by purinergic antagonist PPADS. The amplitude distribution of eEPSCs at minimal stimulation was very different from that seen in the first group of cells, because it exhibited several (typically three) peaks; this changed to a single peak after blockade of glutamate receptors (Fig. 6 B). The initial amplitude distribution was best fit by a compound model with two separate underlying components (Fig. 6 B). The first was single quantal in all 16 cells and had lower release probability and smaller quantal size, similar to the quantal size of the current remaining in CNQX and SYM2081 (component "1," Fig. 6 C). The second component had a larger quantal size and was single quantal in 11 cells ($\alpha < 0.01$) and multiquantal in five cells ($\alpha < 0.05$ for three cells and < 0.1 for two cells; component "2," Fig. 6 C). The mean quantal content of the ATP-mediated and glutamate-mediated components were 0.23 ± 0.9 and 0.82 ± 0.44 ($n = 16$), respectively; the quantal size of these components were 6.2 ± 3.3 pA and 9.1 ± 5.7 pA, respectively ($n = 16$). These values agree with the quantal size of purinergic and glutamatergic EPSCs in the first group of cells.

The value of quantal size in the evoked EPSC gives an estimate for the unitary properties of the synaptic current, whether this corresponds to a single postsynaptic site or a single synaptic vesicle (Auger and Marty, 2000); these estimates can therefore be compared with the properties of the spontaneous mEPSCs. The quantal size of the evoked purinergic EPSC was 74 ± 16% ($n = 35$) of the control evoked EPSC (i.e., before adding glutamate receptor blockers). The corresponding value for the mEPSCs in the same cells was 73 ± 11% ($n = 35$). After glutamate receptor blockade, there was also no difference between the mean amplitude of the unitary evoked EPSC and the spontaneous mEPSC ($P < 0.01$, ANOVA test). These results suggest that both evoked EPSCs and spontaneous ATP-mediated mEPSCs originate from the same synapses.

This conclusion is supported by the effect of changing the intensity of stimulation on ATP-mediated spontaneous currents. We observed that the frequency of ATP-mediated mEPSCs recorded between stimulations was higher when the stronger stimulation was applied (Fig. 5). The increase in the purinergic mEPSC frequency was 91 ± 57% as compared with that recorded in between episodes of minimal stimulation ($n = 8$). This indicates the appearance of new spontaneous events after activation of additional axons/terminals by the stronger stimulus. One feasible explanation for this could be an enhancement of the release due to a residual increase in the background calcium level in the presynaptic terminals after repetitive stimulation. Another explanation might be the recruitment of P2X receptors to the synaptic membrane following the glutamate receptor activation. Whatever the mechanism, the appearance of new spontaneous events suggests that they occur at the same terminals as the evoked currents.

Unitary purinergic currents were observed in ~45% cases of single-fiber (minimal) stimulation and in 100% cases of multifiber (stronger) stimulation. At the same time, the purinergic EPSC was always accompanied by a

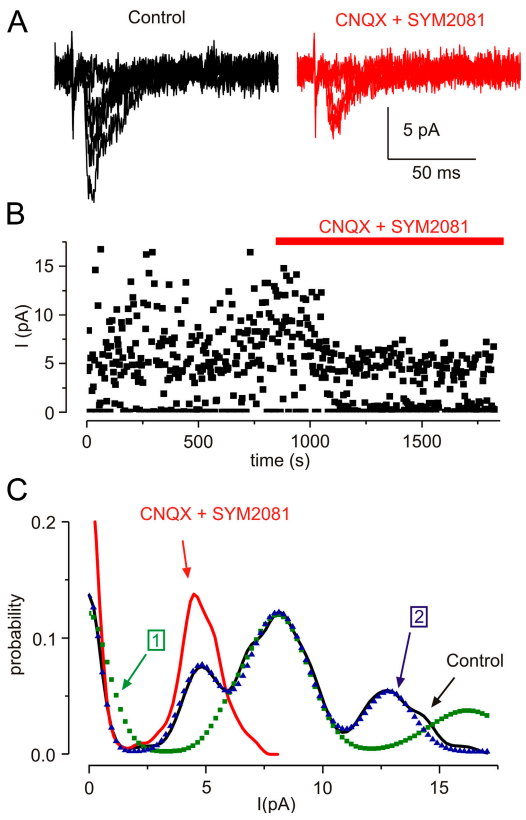

Figure 6. ATP-mediated current evoked at minimal stimulation. (A) EPSCs before and after CNQX (50 μM) and SYM2081 (10 μM). (B) Time course of block by CNQX and SYM2081. (C) Amplitude distribution of EPSCs in control conditions (black line, peaks at 4.7 and 7.9 pA) and in CNQX and SYM2081 (red). Dotted lines are fits of the distributions; binomial with single quantal size (7.9 pA, green dots; component 1) and compound fit with two quantal sizes (4.7 and 7.9 pA, blue triangles; component 2).

glutamate-mediated unitary current; in all 35 cells tested there was no case of a purely purinergic current by single-fiber stimulation. On this ground, the existence of specific purinergic axons seems unlikely. Our result is best ascribed to the vesicular release of ATP at some of the same synapses as glutamate.

We were unable to distinguish between the ATP-mediated eEPSCs (i.e., in 50 μM CNQX and 10 μM SYM2081) and the glutamate-mediated eEPSCs (i.e., in control conditions) by a range of further properties. First, we did not observe any significant difference in the latency of purinergic and glutamatergic evoked synaptic currents. Second, the paired-pulse ratio (see Materials and methods) was 1.01 ± 0.25 (n = 24) for the former, and 1.04 ± 0.21 (n = 16) for the latter (unpublished data); in individual cells the paired-pulse ratio was well correlated for the glutamatergic and purinergic currents ($R > 0.99$, $P < 0.02$). Baclofen (3 μM) decreased the amplitude of the first and second EPSCs, increased the number of failures (zero synaptic responses) and increased the paired-pulse ratio; the effects were the same for both control currents and currents after glutamate receptor blockade. It is well attested that metabotropic glutamate receptors (mGluRs) modulate synaptic strength in glutamatergic synapses (Simkus and Stricker, 2002; Schoepp 2001). In particular, activation of mGluRs group I (which activated $InsP_3$-dependent Ca^{2+} release form intracellular stores) enhances (Simkus and Stricker, 2002), whereas stimulation of mGluRs group III suppresses (Schoepp, 2001) synaptic transmission. We tested the effects of mGluR group III receptor agonist (1S,3R,4S)-1-aminocyclopentane-1,2,4-tricarboxylic acid (ACPT-1; 10 μM; n = 5), which decreased the average amplitudes, increased the number of failures and decreased the paired-pulse ratio for both ATP-mediated and glutamate-mediated events. Finally, α-latrotoxin (330 nM; n = 4) increased the average amplitudes, decreased the failure rate and increased the paired-pulse ratio (unpublished data). All in all, experiments described above did not reveal any significant difference in the behavior of glutamatergic and purinergic EPSCs.

DISCUSSION

The main finding of the present work is that two populations of mEPSC are found in mouse layer 2/3 cortical pyramidal cells. They can be distinguished by their amplitudes and pharmacological properties. The small mEPSCs have about one-half the amplitude of the predominant EPSCs, they persist in very high concentrations of AMPA receptor blockers and agents promoting kainate receptor desensitization, and they are unaffected by cyclothiazide. These small mEPSCs correspond in their properties to a component of the evoked EPSC. They are partially blocked by antagonists of P2X receptors, but firm conclusions about the identity of the underlying P2X receptor are not possible yet. The most abundant P2X receptor subunits in the cortex are $P2X_4$ and $P2X_6$, but others are also present (Collo et al., 1996; Rubio and Soto, 2001). The pharmacological properties of mouse $P2X_4$ receptors do not correspond in detail to those of the mEPSCs. When expressed in HEK 293 cells, homomeric $P2X_4$ receptors are insensitive to suramin (100 μM) but blocked by PPADS (IC_{50} ~10 μM; Jones et al., 2000). The mEPSCs in our experiments were partially blocked by suramin and PPADS, but these are far from reliable antagonists with which to identify the subunit specificity of P2X receptors. Not only are their effects species and subunit dependent, but they also block a range of other ion channels (North and Surprenant, 2000).

In our experiments we used rather moderate concentration of PPADS to ensure washout. In our previous experiments (e.g., Pankratov et al., 1998, 2003) we observed that effects of 10–30 μM of PPDAS were only partially reversible. We considered demonstration of reversible effect of antagonist being more preferable for pharmacological characterization; the interpretation of irreversible block

might be somewhat ambiguous. The IC_{50} of PPADS for different subtypes of P2X receptors lies in the range 1–10 μM (North and Surprenant, 2000), so 3 μM should effectively inhibit P2X-mediated currents. On the other hand, one might not expect complete inhibition of purinergic current in the central nervous system because the $P2X_4$ subunit is most abundant, and receptors containing $P2X_4$ subunits are insensitive to suramin and PPADS (North and Surprenant, 2000).

Another possibility, that the small amplitude mEPSCs results from activation of kainate receptors (Cossart et al., 2002) seems very unlikely in view of their persistence in 50 μM CNQX, or 100 μM NBQX or 10 μM SYM2081. To exclude possible involvement of acetylcholin-mediated transmission, we treated cortical slices with hexametonium. The latter is a classical open-channel blocker (Buisson and Bertrand, 1998), which effectively inhibits nicotinic cholinoreceptors when the cells are kept at hyperpolarized potentials (−80 mV in our case). The absence of any effect of hexamethonium (100 μM) does not fully exclude a contribution from nicotinic receptors, given that it is a relatively weak blocker of some central nicotinic receptors (e.g., α3β4 receptors; Winzer-Serhan and Leslie, 1997; Xiao et al., 1998). These caveats notwithstanding, we proceed on the assumption that the small mEPSCs reflect activation of P2X receptors by ATP.

The ATP seems not to be released with glutamate (as was proposed for cultured CA3 neurones by Mori et al., 2001) or with GABA (as was proposed for cultured lateral hypothalamic neurones by Jo and Role [2002] and spinal neurones by Jo and Schlichter [1999]). In the first case, synchronous release of ATP and glutamate should lead to summation of mEPSCs, which would result in the appearance of the third, large-amplitude peak on the amplitude histogram. However, the mechanism of spontaneous ATP release clearly shares many features with the vesicular release of glutamate (sensitivity to α-latrotoxin, bafilomycin). In the second case, GABA- and ATP-mediated currents could be discriminated at −40 mV (when E_{Cl} was −60 mV) because GABA currents were outward and P2X currents were inward. Obviously, if GABA was coreleased with ATP, the summation of inward and outward current events would lead to their mutual cancellation, hence reducing the overall frequency of mEPSCs. In fact, we did not observe any difference in mEPSC frequency between −80 and −40 mV. On the other hand, our studies of eEPSCs provided no evidence for a pure "purinergic" nerve population. The experiments with paired-pulse inhibition, and the sensitivity to the presynaptic action of ACPT-1 and baclofen, are consistent with the interpretation that ATP is released from glutamate-containing fibers running vertically within the neocortex because thalamocortical inputs are reported to show paired-pulse inhibition (Gil et al., 1999; Reyes and Sakmann, 1999) and to be insensitive to baclofen (Gil et al., 1997).

The analysis of evoked and miniature EPSCs indicates that the amplitude of the unitary event mediated by P2X receptors is about half the size of the unitary event mediated by AMPA receptors (ratio in the range 0.4–0.8), whereas the probability of an ATP-mediated component to the postsynaptic current is lower (ratio in the range 0.1–0.3). Our results also demonstrate that maximal number of quanta of ATP-mediated evoked synaptic current depends on stimulus strength and, therefore, on the number of axons stimulated. The simplest interpretation may therefore be that ATP is released from a distinct vesicle population at a subset of glutamatergic synapses. We cannot say with confidence whether this subset is defined by its ability to release ATP or by the presence of postsynaptic P2X receptors (or both). The latter interpretation would be consistent with the electron microscopic finding that $P2X_4$ subunits are found at about one half of excitatory synapses (in hippocampus and cerebellum; Rubio and Soto, 2001). Alternatively, the ATP may be contained within vesicle with another "cotransmitter" such as a peptide. While considering all the possibilities outlined above we are acutely aware that the present paper does not answer all questions regarding quantal release of ATP, and further understanding of the role on mechanisms of ATP release in central synapses requires additional experimental efforts.

The overall contribution of ATP to the postsynaptic current is small because there is a lower probability of release and/or a lower number of ATP-containing vesicles as compared with those containing glutamate. In fact, the mean quantal content of the purinergic EPSC was three to four times lower than the quantal content of glutamate-mediated EPSC. Given that only some 30–50% of synapses either release ATP or express P2X receptors, one could estimate the relative frequency of ATP-mediated events as 10–30%. This agrees with the relative frequency of purinergic mEPSCs (10–40% of control) as compared with glutamate mEPSCs. Thus, the purinergic excitatory synaptic input is minor in comparison to the glutamatergic input, even though the size of unitary ATP-mediated currents is actually about one half of the magnitude of glutamate-mediated currents. Nevertheless the ATP component can bring heterogeneity to the function of excitatory synapses, given that P2X receptors provide significant calcium entry and that, unlike the case for NMDA receptors, this entry does not require postsynaptic depolarization (Pankratov et al., 2002). The calcium entry itself may strengthen the synaptic connection over the longer term, particularly if the changes in intracellular calcium can bring either P2X or AMPA receptors to the membrane.

This research was supported by The Wellcome Trust.

Olaf S. Andersen served as editor.

Submitted: 6 November 2006
Accepted: 8 February 2007

REFERENCES

Auger, C., and A. Marty. 2000. Quantal currents at single-site central synapses. *J. Physiol.* 526:3–11.

Bardoni, R., P.A. Goldstein, C.J. Lee, J.G. Gu, and A.B. MacDermott. 1997. ATP P2X receptors mediate fast synaptic transmission in the dorsal horn of the rat spinal cord. *J. Neurosci.* 17:5297–5304.

Buisson, B., and D. Bertrand. 1998. Allosteric modulation of neuronal nicotinic acetylcholine receptors. *J. Physiol. (Paris).* 92:89–100.

Burnstock, G., and M.E. Holman. 1961. The transmission of excitation from autonomic nerve to smooth muscle. *J. Physiol.* 155:115–133.

Collo, G., R.A. North, E. Kawashima, E. Merlo-Pich, S. Neidhart, A. Surprenant, and G. Buell. 1996. Cloning of $P2X_5$ and $P2X_6$ receptors and the distribution and properties of an extended family of ATP-gated ion channels. *J. Neurosci.* 16:2495–2507.

Cossart, R., J. Epsztein, R. Tyzio, H. Becq, J. Hirsch, Y. Ben-Ari, and V. Crepel. 2002. Quantal release of glutamate generates pure kainate and mixed AMPA/kainate EPSCs in hippocampal neurons. *Neuron.* 35:147–159.

Edwards, F.A., A.J. Gibb, and D. Colquhoun. 1992. ATP receptor-mediated synaptic currents in the central nervous system. *Nature.* 359:144–147.

Edwards, F.A., S.J. Robertson, and A.J. Gibb. 1997. Properties of ATP receptor-mediated synaptic transmission in the rat medial habenula. *Neuropharmacology.* 36:1253–1268.

Gil, Z., B.W. Connors, and Y. Amitai. 1997. Differential regulation of neocortical synapses by neuromodulators and activity. *Neuron.* 19:679–686.

Gil, Z., B.W. Connors, and Y. Amitai. 1999. Efficacy of thalamocortical and intracortical synaptic connections: quanta, innervation, and reliability. *Neuron.* 23:385–397.

Jo, Y.H., and L.W. Role. 2002. Coordinate release of ATP and GABA at in vitro synapses of lateral hypothalamic neurons. *J. Neurosci.* 22:4794–4804.

Jo, Y.H., and R. Schlichter. 1999. Synaptic corelease of ATP and GABA in cultured spinal neurons. *Nat. Neurosci.* 2:241–245.

Jones, C.A., I.P. Chessell, J. Simon, E.A. Barnard, K.J. Miller, A.D. Michel, and P.P. Humphrey. 2000. Functional characterization of the $P2X_4$ receptor orthologues. *Br. J. Pharmacol.* 129:388–394.

Katz, B., and R. Miledi. 1963. A study of spontaneous miniature potentials in spinal motoneurones. *J. Physiol.* 168:389–422.

Khakh, B.S. 2001. Molecular physiology of P2X receptors and ATP signalling at synapses. *Nat. Rev. Neurosci.* 2:165–174.

Mori, M., C. Heuss, B.H. Gahwiler, and U. Gerber. 2001. Fast synaptic transmission mediated by P2X receptors in CA3 pyramidal cells of rat hippocampal slice cultures. *J. Physiol.* 535:115–123.

Nieber, K., W. Poelchen, and P. Illes. 1997. Role of ATP in fast excitatory synaptic potentials in locus coeruleus neurones of the rat. *Br. J. Pharmacol.* 122:423–430.

Norenberg, W., and P. Illes. 2000. Neuronal P2X receptors: localisation and functional properties. *Naunyn Schmiedebergs Arch. Pharmacol.* 362:324–339.

North, R.A. 2002. Molecular physiology of P2X receptors. *Physiol. Rev.* 82:1013–1067.

North, R.A., and A. Surprenant. 2000. Pharmacology of cloned P2X receptors. *Annu. Rev. Pharmacol. Toxicol.* 40:563–580.

North, R.A., and A. Verkhratsky. 2006. Purinergic transmission in the central nervous system. *Pflugers Arch.* 452:479–485.

Pankratov, Y.V., and O.A. Krishtal. 2003. Distinct quantal features of AMPA and NMDA synaptic currents in hippocampal neurons: implication of glutamate spillover and receptor saturation. *Biophys. J.* 85:3375–3387.

Pankratov, Y., E. Castro, M.T. Miras-Portugal, and O. Krishtal. 1998. A purinergic component of the excitatory postsynaptic current mediated by P2X receptors in the CA1 neurons of the rat hippocampus. *Eur. J. Neurosci.* 10:3898–3902.

Pankratov, Y., U. Lalo, O. Krishtal, and A. Verkhratsky. 2002. Ionotropic P2X purinoreceptors mediate synaptic transmission in rat pyramidal neurones of layer II/III of somato-sensory cortex. *J. Physiol.* 542:529–536.

Pankratov, Y., U. Lalo, O. Krishtal, and A. Verkhratsky. 2003. P2X receptor-mediated excitatory synaptic currents in somatosensory cortex. *Mol. Cell. Neurosci.* 24:842–849.

Partin, K.M., D.K. Patneau, C.A. Winters, M.L. Mayer, and A. Buonanno. 1993. Selective modulation of desensitization at AMPA versus kainate receptors by cyclothiazide and concanavalin A. *Neuron.* 11:1069–1082.

Pearson, R.A., N. Dale, E. Llaudet, and P. Mobbs. 2005. ATP released via gap junction hemichannels from the pigment epithelium regulates neural retinal progenitor proliferation. *Neuron.* 46:731–744.

Redman, S. 1990. Quantal analysis of synaptic potentials in neurons of the central nervous system. *Physiol. Rev.* 70:165–198.

Rettinger, J., G. Schmalzing, S. Damer, G. Muller, P. Nickel, and G. Lambrecht. 2000. The suramin analogue NF279 is a novel and potent antagonist selective for the $P2X_1$ receptor. *Neuropharmacology.* 39:2044–2053.

Reyes, A., and B. Sakmann. 1999. Developmental switch in the short-term modification of unitary EPSPs evoked in layer 2/3 and layer 5 pyramidal neurons of rat neocortex. *J. Neurosci.* 19:3827–3835.

Rubio, M.E., and F. Soto. 2001. Distinct localization of P2X receptors at excitatory postsynaptic specializations. *J. Neurosci.* 21:641–653.

Schoepp, D.D. 2001. Unveiling the functions of presynaptic metabotropic glutamate receptors in the central nervous system. *J. Pharmacol. Exp. Ther.* 299:12–20.

Simkus, C.R., and C. Stricker. 2002. The contribution of intracellular calcium stores to mEPSCs recorded in layer II neurones of rat barrel cortex. *J. Physiol.* 545:521–535.

Sperlagh, B., and E.S. Vizi. 2001. Regulation of purine release. *In* Purinergic and Pyrimidinergic Signalling. M.P. Abbraccio and M. Williams, editors. Springer Verlag, Berlin. 179–208.

Stricker, C., A.C. Field, and S.J. Redman. 1996a. Changes in quantal parameters of EPSCs in rat CA1 neurones in vitro after the induction of long-term potentiation. *J. Physiol.* 490:443–454.

Stricker, C., A.C. Field, and S.J. Redman. 1996b. Statistical analysis of amplitude fluctuations in EPSCs evoked in rat CA1 pyramidal neurones in vitro. *J. Physiol.* 490:419–441.

Ushkaryov, Y.A., K.E. Volynski, and A.C. Ashton. 2004. The multiple actions of black widow spider toxins and their selective use in neurosecretion studies. *Toxicon.* 43:527–542.

Verkhratsky, A., R.K. Orkand, and H. Kettenmann. 1998. Glial calcium: homeostasis and signaling function. *Physiol. Rev.* 78:99–141.

Verkhratsky, A., and C. Steinhauser. 2000. Ion channels in glial cells. *Brain Res. Brain Res. Rev.* 32:380–412.

Winzer-Serhan, U.H., and F.M. Leslie. 1997. Codistribution of nicotinic acetylcholine receptor subunit $\alpha 3$ and $\beta 4$ mRNAs during rat brain development. *J. Comp. Neurol.* 386:540–554.

Xiao, Y., E.L. Meyer, J.M. Thompson, A. Surin, J. Wroblewski, and K.J. Kellar. 1998. Rat $\alpha 3/\beta 4$ subtype of neuronal nicotinic acetylcholine receptor stably expressed in a transfected cell line: pharmacology of ligand binding and function. *Mol. Pharmacol.* 54:322–333.

Yoshimura, Y., H. Sato, K. Imamura, and Y. Watanabe. 2000. Properties of horizontal and vertical inputs to pyramidal cells in the superficial layers of the cat visual cortex. *J. Neurosci.* 20:1931–1940.

Zhou, Q., C.C. Petersen, and R.A. Nicoll. 2000. Effects of reduced vesicular filling on synaptic transmission in rat hippocampal neurones. *J. Physiol.* 525:195–206.